Final-state interactions in the response of nuclear matter

M. Petraki,[1] E. Mavrommatis,[1] O. Benhar,[2] J. W. Clark,[3] A. Fabrocini,[4] and S. Fantoni[5]
[1]*Physics Department, Division of Nuclear and Particle Physics, University of Athens, GR-15771 Athens, Greece*
[2]*INFN, Sezione di Roma 1, I-00185 Roma, Italy*
[3]*Physics Department, Washington University, St. Louis MO 63130*
[4]*Department of Physics "E. Fermi," University of Pisa, and INFN, Sezione di Pisa, I-56100 Pisa, Italy*
[5]*International School for Advanced Studies (SISSA), I-30014 Trieste, Italy*
(Received 8 January 2002; published 27 January 2003)

Final-state interactions in the response of a many-body system to an external probe delivering large momentum are normally described using the eikonal approximation, for the trajectory of the struck particle, and the frozen approximation, for the positions of the spectators. We propose a generalization of this scheme, in which the initial momentum of the struck particle is explicitly taken into account. Numerical calculations of the nuclear matter response at $1<|\mathbf{q}|<2$ GeV/c show that the inclusion of this momentum dependence leads to a sizable effect in the low-energy tail. Possible implications for the analysis of existing electron-nucleus scattering data are discussed.

DOI: 10.1103/PhysRevC.67.014605 PACS number(s): 21.65.+f, 25.30.Fj, 25.30.Rw

I. INTRODUCTION

Final-state interactions (FSI's) of fast nucleons produced in electron-nucleus scattering at large momentum transfer have long been known to exert a significant effect on the coincidence $(e,e'p)$ cross section; moreover, they provide most of the strength observed in the low-energy loss tail of the inclusive (e,e') cross section (see, e.g., Ref. [1]). The main effect of FSI's is a damping of the motion of the struck particle, which can be qualitatively described in terms of the imaginary part of the nuclear optical potential. However, since nucleons in nuclei are strongly correlated, one must improve upon the optical potential approach rooted in a simple mean-field description of nuclear dynamics, if one hopes to develop a fully quantitative treatment of FSI's. It is very important to realize that nucleon-nucleon (NN) correlations, leading to large density fluctuations and to the appearance of high momentum components in the nuclear wave function, strongly affect both initial and final states in electron-nucleus scattering, and must be consistently taken into account.

A theoretical description of (e,e') processes including correlation effects was developed in Ref. [2] (hereafter referred to as I) and successfully employed to analyze (e,e') data for momentum transfer in the range 1 GeV/$c<|\mathbf{q}|<2$ GeV/c [2–4]. A similar approach, formulated in analogy with the theoretical treatment of FSI's in neutron scattering from quantum liquids, was proposed in Ref. [5].

The treatment of FSI's discussed in I, commonly referred to as correlated glauber approximation (CGA), rests on the assumptions that (i) the struck nucleon moves along a straight line with a constant velocity (eikonal approximation), and (ii) the spectator nucleons are seen by the fast struck particle as a collection of fixed scattering centers (frozen approximation). The resulting inclusive cross section can be written as a convolution integral, involving the cross section evaluated within the plane-wave impulse approximation (PWIA), i.e., evaluated in the absence of FSI's, and a folding function embodying FSI effects. The CGA entails the same set of approximations as the Glauber theory of high-energy proton scattering off nuclei [6], which has been successfully applied for over 40 years. The eikonal and frozen approximations have also been used, in a somewhat different context, to analyze semi-inclusive and exclusive electron-nucleus processes [7,8]

The results of I show that FSI's produce a huge enhancement of the inclusive cross section in the region of $\omega \ll \omega_{QE}$, where ω_{QE} is the energy transfer corresponding to elastic scattering off an isolated stationary nucleon. While this enhancement brings theory and experiment into agreement over a broad range in ω, the calculated cross section substantially overestimates the data in the extreme low-ω tail [roughly corresponding to values of the Bjorken scaling variable $x=(Q^2/2m\omega)>2$, where $Q^2=|\mathbf{q}|^2-\omega^2$, and m denotes the nucleon mass]. In order to reproduce the tail of the measured cross sections, the imaginary part of the free-space NN scattering amplitude, which determines the shape of the CGA folding function, must be modified in such a way as to reduce the effect of FSI's.

As pointed out in I, NN scattering in the nuclear medium may in principle differ markedly from scattering in free space. For example, Pauli blocking and dispersive corrections are known to be important at moderate energies [9]. However, their effects on the calculated cross sections have been found to be small in the kinematical region spanned by the data analyzed in Refs. [2–4]. Corrections to the NN amplitude associated with the extrapolation to off-shell energies are also expected to be small [10].

A different type of modification of the NN cross section, originating from the internal structure of the nucleon, may play a more significant role. It was suggested [11,12] that elastic scattering on a nucleon at high momentum transfer can only occur if the nucleon is found in the Fock state having the lowest number of constituents, so that the momentum transfer can be most effectively shared among them. Within this picture, a nucleon is in a very compact configuration after absorbing a large momentum $\mathbf{q}$. It then travels through nuclear matter experiencing very few FSI's, until its

standard size is recovered on a characteristic time scale that increases with $|\mathbf{q}|$. In the limit of infinite momentum transfer, FSI's are totally suppressed, and the nuclear medium is said to exhibit *color transparency*.

The results of the calculations of Refs. [2–4] show that inclusion of the effects of color transparency according to the model of Ref. [13], *with no adjustable parameters*, greatly improves the agreement between theory and data, yielding a satisfactory description of the low-energy loss tail of the nuclear inclusive cross sections for $Q^2 > 1.5$ $(\mathrm{GeV}/c)^2$.

To firmly establish the occurrence of color transparency in (e,e') processes, the accuracy of the approximations underlying the CGA must be carefully investigated and either validated or transcended. In this paper, we introduce a treatment of FSI's which improves upon the CGA, in that it allows one to take account of the initial momentum of the struck nucleon. Within this approach, the response can no longer be written as a simple convolution integral. However, it can still be expressed in terms of the spectral function and a generalized folding function, in a form displaying explicit dependence on both the initial and final momenta of the struck particle.

The theoretical description of nuclear-matter response is discussed in Section II, where we outline the development of a systematic scheme that improves upon the PWIA and includes FSI effects. The details of the many-body calculation of the generalized folding function within the Fermi hypernetted chain (FHNC) approach are traced in Sec. III. The ensuing numerical results are presented and analyzed in Sec. IV, with particular attention to the generalized folding functions and the nuclear matter *y*-scaling functions at different values of $|\mathbf{q}|$. Section V summarizes our findings and states our conclusions.

II. NUCLEAR-MATTER RESPONSE

A. Plane-wave impulse approximation

The analysis carried out in Refs. [2–4] required a full calculation of the nuclear cross section, including the electromagnetic vertex, as well as the use of spectral functions adapted to finite targets (such as those obtained within a local-density approximation [4]). In addition, since the typical momentum transfers lie in the 1–2-GeV/c range, consistent use of relativistic kinematics was essential.

In this paper, we will avoid these complications and focus on the nonrelativistic response of infinite nuclear matter to a scalar probe, defined by

$$S(\mathbf{q},\omega) = \frac{1}{A}\int \frac{dt}{2\pi} e^{i\omega t}\langle 0|\rho_{\mathbf{q}}^{\dagger}(t)\rho_{\mathbf{q}}(0)|0\rangle = \frac{1}{A}\int \frac{dt}{2\pi} e^{i(\omega+E_0)t}\langle 0|\rho_{\mathbf{q}}^{\dagger} e^{-iHt}\rho_{\mathbf{q}}|0\rangle. \quad (1)$$

Here H and $|0\rangle$ denote the nuclear Hamiltonian and the corresponding ground state satisfying the Schrödinger equation $H|0\rangle = E_0|0\rangle$. The time-dependent density fluctuation operator $\rho_{\mathbf{q}}(t)$ is constructed as

$$\rho_{\mathbf{q}}(t) = e^{iHt}\rho_{\mathbf{q}}e^{-iHt} = e^{iHt}\sum_{\mathbf{k}} a_{\mathbf{k}+\mathbf{q}}^{\dagger}a_{\mathbf{k}}e^{-iHt}, \quad (2)$$

where $a_{\mathbf{k}}^{\dagger}$ and $a_{\mathbf{k}}$ are nucleon creation and annihilation operators, respectively. Note that the definition given in Eq. (1) can be readily generalized to describe the electromagnetic response by replacing $\rho_{\mathbf{q}}$ with the appropriate current operator.

Retaining only the incoherent contribution to the response, which is known to be dominant at large $|\mathbf{q}|$, Eq. (1) can be rewritten in the form

$$S(\mathbf{q},\omega) = \int \frac{dt}{2\pi} e^{i(\omega+E_0)t}\hat{S}(\mathbf{q},t), \quad (3)$$

with

$$\hat{S}(\mathbf{q},t) = \int dR dR' \Psi_0^*(R') e^{-i\mathbf{q}\cdot\mathbf{r}_1'} \times \langle R'|e^{-iHt}|R\rangle e^{i\mathbf{q}\cdot\mathbf{r}_1}\Psi_0(R), \quad (4)$$

where $\{R\} = \{\mathbf{r}_1, \mathbf{r}_2, \ldots, \mathbf{r}_A\}$ specifies the spatial configuration of the A-nucleon system, $\Psi_0(R) = \langle R|0\rangle$ is its ground-state wave function, and the propagator $U_A(R,R';t) = \langle R'|e^{-iHt}|R\rangle$ represents the amplitude for the system to evolve from configuration R to configuration R' during a time t. The wave function $\Psi_0(R)$ can in principle be evaluated within nonrelativistic nuclear many-body theory. On the other hand, the nonrelativistic approach cannot be used to obtain the A-particle propagator $U_A(R,R';t)$, since—in the kinematical regime under consideration—the struck nucleon typically carries a momentum larger than the nucleon mass. In view of the fact that a fully realistic and consistent calculation of $U_A(R,R';t)$ remains intractable, one must resort to simplifying assumptions.

A systematic approximation scheme can be developed by first decomposing the Hamiltonian according to

$$H = H_{A-1} + T_1 + H_I, \quad (5)$$

where $H_{\mathrm{A}-1}$ is the nonrelativistic Hamiltonian of the *fully interacting* $(A-1)$-particle spectator system and T_1 denotes the Hamiltonian describing a *free* nucleon. The term

$$H_I = \sum_{j=2}^{A} v_{1j}, \quad (6)$$

where v_{ij} is the NN potential, accounts for the interactions between the struck particle and the spectators.

The PWIA amounts to setting $H_I = 0$ in Eq. (5), thus disregarding FSI's altogether, and neglecting Pauli blocking of the states available to the high-energy struck nucleon. The resulting A-particle propagator factorizes into the product of the interacting $(A-1)$-particle propagator and the free-space one-body propagator describing the struck nucleon,

$$U_{\rm PWIA}(R,R';t)=\langle\tilde{R}'|e^{-iH_{A-1}t}|\tilde{R}\rangle\langle\mathbf{r}_1'|e^{-iT_1t}|\mathbf{r}_1\rangle$$
$$=U_{A-1}(\tilde{R},\tilde{R}';t)U_0(\mathbf{r}_1,\mathbf{r}_1';t), \qquad (7)$$

where $\{\tilde{R}\}=\{\mathbf{r}_2,\ldots,\mathbf{r}_A\}$ specifies the configuration of the spectator system. Equation (7) clearly shows that within the PWIA, nuclear dynamics only appears through U_{A-1}, while the treatment of the relativistic motion of the struck nucleon reduces to a trivial kinematic problem.

We next express the PWIA $S(\mathbf{q},t)$ (and thereby the response) in terms of the nucleon spectral function $P(\mathbf{k},E)$, which by definition gives the probability of removing a nucleon with momentum $\mathbf{k}$ from the nuclear ground state, leaving the residual system with excitation energy E. Introducing spectral representations for both U_{A-1} and U_0 (see, e.g., Ref. [14]), we obtain

$$\hat{S}_{\rm PWIA}(\mathbf{q},t)=\int\frac{d^3p}{(2\pi)^3}\int dEP(\mathbf{p}-\mathbf{q},E)e^{-i(E-E_0+E_p)t}, \qquad (8)$$

which leads to the familiar result [14]

$$S_{\rm PWIA}(\mathbf{q},\omega)=\int\frac{d^3p}{(2\pi)^3}\int dEP(\mathbf{p}-\mathbf{q},E)\,\delta(\omega-E-E_p), \qquad (9)$$

where $E_p=|\mathbf{p}|^2/2m$ denotes the kinetic energy of a nucleon carrying momentum $\mathbf{p}$.

B. Inclusion of final-state effects

In order to improve upon the PWIA, one needs to devise a set of sensible approximations to treat the contributions to the A-particle propagator coming from the FSI Hamiltonian H_I. As a first step, we make the replacement

$$e^{-i(H_{A-1}+T_1+H_I)t}\rightarrow e^{-iH_{A-1}t}e^{-i(T_1+H_I)t}, \qquad (10)$$

which essentially amounts to assuming that the internal dynamics of the spectator system and its FSI with the struck particle do not affect one another, and can therefore be completely decoupled. Within this picture, the spectator system evolves during the time t as if there were no struck particle moving around, while the fast struck particle ''sees'' the spectator system as if it were *frozen* at time $t=0$.

Under this assumption, which implies that the configuration of the spectator system does not change due to interactions with the fast struck nucleon, we can use completeness of the $(A-1)$-particle position eigenstates to rewrite the propagator in the simple factorized form

$$U_A(R,R';t)=\int d\tilde{R}''\langle\tilde{R}'|e^{-iH_{A-1}t}|\tilde{R}''\rangle$$
$$\times\langle\mathbf{r}_1',\tilde{R}'|e^{-i(T_1+H_I)t}|\mathbf{r}_1,\tilde{R}\rangle$$
$$=U_{A-1}(\tilde{R},\tilde{R}';t)\langle\mathbf{r}_1',\tilde{R}|e^{-i(T_1+H_I)t}|\mathbf{r}_1,\tilde{R}\rangle$$
$$=U_{A-1}(\tilde{R},\tilde{R}';t)U_1(\mathbf{r}_1\tilde{R},\mathbf{r}_1'\tilde{R};t). \qquad (11)$$

An evaluation of $U_1(\mathbf{r}_1\tilde{R},\mathbf{r}_1'\tilde{R};t)$ in general requires a functional integration over the set of trajectories $\mathbf{r}_1(\tau)$ satisfying the boundary conditions $\mathbf{r}_1(0)=\mathbf{r}_1$ and $\mathbf{r}_1(t)=\mathbf{r}_1'$ (see, e.g., Ref. [15]). However, for large momenta of the struck nucleon, the evaluation can be drastically simplified by invoking the *eikonal approximation*, i.e., by assuming that the particle moves along a straight trajectory with constant velocity $\mathbf{v}=(\mathbf{r}_1'-\mathbf{r}_1)/t$, so that $\mathbf{r}_1(\tau)=\mathbf{r}_1+\mathbf{v}\tau$. Within this approximation, the propagator $U_1(\mathbf{r}_1\tilde{R},\mathbf{r}_1'\tilde{R};t)$ takes the factorized form [16]

$$U_1(\mathbf{r}_1\tilde{R},\mathbf{r}_1'\tilde{R};t)=U_0(\mathbf{r}_1,\mathbf{r}_1';t)U_{\mathbf{p}}(\mathbf{r}_1,\tilde{R};t), \qquad (12)$$

where the eikonal propagator $U_{\mathbf{p}}(\mathbf{r}_1,\tilde{R};t)$ is given by

$$U_{\mathbf{p}}(\mathbf{r}_1,\tilde{R};t)=\exp\left[-i\int_0^t d\tau\sum_{j=2}^{A}v(\mathbf{r}_1+\mathbf{v}\tau-\mathbf{r}_j)\right], \qquad (13)$$

v being the NN potential and $U_0(\mathbf{r}_1,\mathbf{r}_1';t)$ the free-space nucleon propagator.

Expanding the exponential appearing in the right-hand side of Eq. (13), one obtains a series whose terms are associated with processes involving an increasing number of interactions between the struck nucleon and the spectators. The terms corresponding to repeated interactions with the same spectator can be summed up to all orders by replacing the bare NN interaction v with the coordinate space t-matrix $\Gamma_{\mathbf{q}}(\mathbf{r})$, which is related to the NN scattering amplitude $f_{\mathbf{q}}(\mathbf{k})$ at incident momentum $\mathbf{q}$ and momentum transfer $\mathbf{k}$ through

$$\Gamma_{\mathbf{q}}(\mathbf{r})=-\frac{2\pi}{m}\int\frac{d^3k}{(2\pi)^3}e^{i\mathbf{k}\cdot\mathbf{r}}f_{\mathbf{q}}(\mathbf{k}). \qquad (14)$$

Using the above results together with spectral representations of both $U_0(\mathbf{r}_1,\mathbf{r}_1';t)$ and $U_{A-1}(\tilde{R},\tilde{R}';t)$, the response can finally be expressed as

$$S(\mathbf{q},\omega)=\int\frac{dt}{2\pi}e^{i(\omega+E_0)t}\int\frac{d^3p}{(2\pi)^3}e^{-iE_pt}$$
$$\times\sum_n e^{-iE_nt}M_{0n}^*(\mathbf{p}-\mathbf{q})\tilde{M}_{0n}(\mathbf{p},\mathbf{q};t), \qquad (15)$$

where the sum extends over the $(A-1)$-particle states satisfying the Schrödinger equations $H_{A-1}|n\rangle=E_n|n\rangle$. We have introduced the definitions

$$M_{0n}(\mathbf{k})=\int dRe^{i\mathbf{k}\cdot\mathbf{r}_1}\Psi_0^*(R)\Phi_n(\tilde{R}), \qquad (16)$$

with $\Phi_n(\tilde{R})=\langle\tilde{R}|n\rangle$, and

$$\tilde{M}_{0n}(\mathbf{p},\mathbf{q};t)=\int dRe^{-i(\mathbf{p}-\mathbf{q})\cdot\mathbf{r}_1}\Phi_n^*(\tilde{R})\Psi_0(R)U_{\mathbf{p}}(\mathbf{r}_1,\tilde{R};t). \qquad (17)$$

In the limit $U_{\mathbf{p}}(\mathbf{r}_1,\tilde{R};t)\rightarrow 1$, we have $\tilde{M}_{0n}(\mathbf{p},\mathbf{q};t)\rightarrow M_{0n}(\mathbf{p}-\mathbf{q})$, and the response $S(\mathbf{q},\omega)$ given by Eq. (15) reduces to the PWIA result.

It is to be emphasized that the calculation of the response according to Eq. (15) involves only two approximations: (i) the frozen approximation for the configuration of the spectator system, and (ii) the eikonal approximation for the trajectory of the struck particle. An explicit calculation of the relevant $\tilde{M}_{0n}(\mathbf{p},\mathbf{q};t)$ integrals within nonrelativistic many-body theory appears to be feasible, at least for few-nucleon systems and infinite nuclear matter. However, to establish a clear connection with the PWIA picture, it is useful to devise approximations that permit $S(\mathbf{q},\omega)$ of Eq. (15) to be expressed in terms of either the spectral function $P(\mathbf{k},E)$ or the PWIA response $S_{\rm PWIA}(\mathbf{q},\omega)$.

The definition of the spectral function,

$$P(\mathbf{k},E)=\sum_n |M_{0n}(\mathbf{k})|^2\delta(E+E_0-E_n), \tag{18}$$

can be recovered in Eq. (15) under the assumption that the integrals $\tilde{M}_{0n}$ of Eq. (17) take the form

$$\tilde{M}_{0n}(\mathbf{p},\mathbf{q};t)=M_{0n}(\mathbf{p}-\mathbf{q})\mathcal{U}(\mathbf{p},\mathbf{q};t), \tag{19}$$

where the function $\mathcal{U}$ is to be independent of the state of the spectator system, labeled by the index n. An even more drastic simplification is achieved upon requiring that the time dependence of $\tilde{M}_{0n}(\mathbf{p},\mathbf{q};t)$ be factorizable according to

$$\tilde{M}_{0n}(\mathbf{p},\mathbf{q};t)=M_{0n}(\mathbf{p}-\mathbf{q})\overline{U}_{\mathbf{q}}(t), \tag{20}$$

i.e., upon assuming that the function $\mathcal{U}$ defined by Eq. (19) does not depend upon $\mathbf{p}$, which in turn corresponds to making the approximation $\mathbf{p}\simeq\mathbf{q}$ in $\mathcal{U}$.

Substitution of Eq. (20) into Eq. (15) allows one to rewrite the response as a convolution integral,

$$S(\mathbf{q},\omega)=\int d\omega' S_{\rm PWIA}(\mathbf{q},\omega')F_{\mathbf{q}}(\omega-\omega'), \tag{21}$$

the folding function $F_{\mathbf{q}}(\omega)$ being given by

$$F_{\mathbf{q}}(\omega)=\int \frac{dt}{2\pi}e^{i\omega t}\overline{U}_{\mathbf{q}}(t). \tag{22}$$

To obtain the function $\overline{U}_{\mathbf{q}}(t)$ embodying all FSI effects [*N.B.* the PWIA can be regained by setting $\overline{U}_{\mathbf{q}}(t)\equiv 1$, i.e., $F(\omega)=\delta(\omega)$], one makes the replacement

$$\sum_{j=2}^{A}\Gamma_{\mathbf{q}}(\mathbf{r}_1+\mathbf{v}\tau-\mathbf{r}_j)\rightarrow\frac{\int dR|\Psi_0(R)|^2\sum_{j=2}^{A}\Gamma_{\mathbf{q}}(\mathbf{r}_1+\mathbf{v}\tau-\mathbf{r}_j)}{\int dR|\Psi_0(R)|^2}$$

$$=\overline{V}_{\mathbf{q}}(\tau), \tag{23}$$

which amounts to averaging FSI's with ground-state configuration weights. In infinite nuclear matter at uniform density ρ, the average involved in Eq. (23) takes the simple form

$$\overline{V}_{\mathbf{q}}(\tau)=\rho\int d^3r g(r)\Gamma_{\mathbf{q}}(\mathbf{r}+\mathbf{v}\tau), \tag{24}$$

where the radial distribution function $g(r)$ measures the probability of finding two nucleons separated by a distance $r=|\mathbf{r}|$. Keeping only the contributions associated with the imaginary part of the NN amplitude, which is known to be dominant at large incident momentum, we can finally write the eikonal propagator as

$$\overline{U}_{\mathbf{q}}(t)=\exp\int d\tau\,\mathrm{Im}\,\overline{V}_{\mathbf{q}}(\tau). \tag{25}$$

The approach developed in I and employed in Refs. [2–4] is based on the assumptions underlying Eqs. (20)–(25). In Ref. [17] the Euclidean response of a nonrelativistic model of the ^{4}He nucleus obtained within this approach was compared to the results of an exact Green's-function Monte Carlo calculation. The close agreement between the two responses suggests that the approximations employed in I are indeed quite reasonable.

A different approximation scheme leading to the factorization of $\tilde{M}_{0n}$ can be obtained by inserting into Eq. (17) the identity

$$\int d\tilde{R}'d^3r_1'\delta(\mathbf{r}_1-\mathbf{r}_1')\delta^{3(A-1)}(\tilde{R}-\tilde{R}')$$

$$=\sum_N\int dR'\Psi_N^*(R')\Psi_N(R), \tag{26}$$

where the sum includes a complete set of eigenstates of the A-particle Hamiltonian H. This procedure is not unique, because the δ-function insertion allows for different assignments of the arguments of the functions entering the right-hand side of Eq. (17), leading to different but ultimately equivalent representations. By equating two such representations, exploiting translation invariance of infinite nuclear matter and retaining only the term corresponding to $|N\rangle=|0\rangle$ we obtain

$$\tilde{M}_{0n}(\mathbf{p},\mathbf{q};t)=M_{0n}(\mathbf{k})\frac{\mathcal{U}_0(\mathbf{k},\mathbf{p};t)}{n(\mathbf{k})}. \tag{27}$$

Here $n(\mathbf{k})$ is the nucleon momentum distribution, defined in terms of the spectral function as

$$n(\mathbf{k})=\int dEP(\mathbf{k},E), \tag{28}$$

while

$$\mathcal{U}_0(\mathbf{k},\mathbf{p};t)=\int d^3r_{11'}e^{i\mathbf{k}\cdot\mathbf{r}_{11'}}\mathcal{P}(\mathbf{p},\mathbf{r}_{11'};t), \tag{29}$$

with $\mathbf{r}_{11'}=\mathbf{r}_1-\mathbf{r}_{1'}$ and

$$\mathcal{P}(\mathbf{p},\mathbf{r}_{11'};t)=\int d\tilde{R}\Psi_0^*(\mathbf{r}_1',\tilde{R})\Psi_0(\mathbf{r}_1,\tilde{R})U_{\mathbf{p}}(\mathbf{r}_1,\tilde{R};t). \tag{30}$$

It can be readily seen that if $U_{\mathbf{p}}(\tilde{R},\mathbf{r}_1;t)\equiv 1$, i.e., if FSI's are absent, the function $\mathcal{P}(\mathbf{p},\mathbf{r}_{11'};t)$ reduces to $\rho(\mathbf{r}_1;\mathbf{r}_{1'})/A$, where

$$\rho_1(\mathbf{r}_1;\mathbf{r}_1')=A\int d\tilde{R}\Psi_0^*(\mathbf{r}_1',\tilde{R})\Psi_0(\mathbf{r}_1,\tilde{R}) \tag{31}$$

is the one-body density matrix, whose Fourier transform is $n(\mathbf{k})$. As a consequence, we have $\tilde{M}_{0n}(\mathbf{p},\mathbf{q};t)=M_{0n}(\mathbf{k})$ and the PWIA is recovered.

Relation (27) can be shown to hold as an equality at the lowest order of the cluster expansion, that is known to provide accurate estimates of a number of nuclear matter properties at equilibrium density (see, e.g., Ref. [18]).

Substitution of Eq. (27) into the definition of the response leads to

$$S(\mathbf{q},\omega)=\int d\omega'\int\frac{d^3k}{(2\pi)^3}F_{\mathbf{k},\mathbf{q}}(\omega'-\omega)\int dEP(\mathbf{k},E)\times\delta(\omega'-E-E_{|\mathbf{k}+\mathbf{q}|}), \tag{32}$$

where the generalized folding function $F_{\mathbf{k},\mathbf{q}}(\omega)$ is defined as

$$F_{\mathbf{k},\mathbf{q}}(\omega)=\frac{1}{n(\mathbf{k})}\int\frac{dt}{2\pi}\,\mathrm{e}^{i\omega t}\mathcal{U}_0(\mathbf{k},\mathbf{k}+\mathbf{q};t). \tag{33}$$

III. MANY-BODY CALCULATION OF THE GENERALIZED FOLDING FUNCTION

Equations (29) and (30) show that calculation of the generalized folding function of Eq. (33) requires a knowledge of the partially diagonal n-body density matrices

$$\rho_n(\mathbf{r}_1,\mathbf{r}_2,\ldots,\mathbf{r}_n;\mathbf{r}_1',\mathbf{r}_2,\ldots,\mathbf{r}_n)=\frac{A!}{(A-n)!}\int d^3r_{n+1}\ldots d^3r_A\Psi_0^*(\mathbf{r}_1',\tilde{R})\Psi_0(\mathbf{r}_1,\tilde{R}) \tag{34}$$

of the target nucleus, for all $n\leqslant A$. The numerical calculation of ρ_n within an *ab initio* microscopic approach involves prohibitive difficulties, even for the case of infinite nuclear matter considered here. In view of this problem, we need to model ρ_n in terms of quantities that consistently incorporate the relevant physics and can still be reliably calculated. The results presented in this paper have been obtained using an approximation scheme (hereafter referred to as the *hole approximation*), in which ρ_n is written in terms of the one-body density matrix: of Eq. (31) and the half-diagonal two-body density matrix

$$\rho_2(\mathbf{r}_1,\mathbf{r}_2;\mathbf{r}_1',\mathbf{r}_2)=A(A-1)\int d^3r_3\ldots d^3r_A\Psi_0^*(\mathbf{r}_1',\tilde{R})\Psi_0(\mathbf{r}_1,\tilde{R}). \tag{35}$$

The explicit formula for the resulting n-body density matrix,

$$\rho_n^{\mathrm{HA}}(\mathbf{r}_1,\mathbf{r}_2,\ldots,\mathbf{r}_n;\mathbf{r}_1',\mathbf{r}_2,\ldots,\mathbf{r}_n)=\frac{1}{[\rho_1(\mathbf{r}_1;\mathbf{r}_1')]^{n-2}}\prod_{i=2}^{n}\rho_2(\mathbf{r}_1,\mathbf{r}_i;\mathbf{r}_1',\mathbf{r}_i), \tag{36}$$

shows that the hole approximation represents the multinucleon spatial correlations involved in the definition of ρ_n as a superposition of two-nucleon correlations.

Among other expressions that can be constructed from the same building blocks, Eq. (36) was chosen primarily because it fulfills some basic properties of the exact density matrices. In particular, ρ_n^{HA}, which is obviously real, satisfies exactly the asymptotic factorization requirement

$$\lim_{|\mathbf{r}_n|\to\infty}\rho_n(\mathbf{r}_1,\mathbf{r}_2,\ldots,\mathbf{r}_n;\mathbf{r}_1',\mathbf{r}_2,\ldots,\mathbf{r}_n)=\rho\rho_{n-1}(\mathbf{r}_1,\mathbf{r}_2,\ldots,\mathbf{r}_{n-1};\mathbf{r}_1',\mathbf{r}_2,\ldots,\mathbf{r}_{n-1}), \tag{37}$$

while violating, although not severely, the sequential relation

$$\int d^3r_n\rho_n(\mathbf{r}_1,\mathbf{r}_2,\ldots,\mathbf{r}_n;\mathbf{r}_1',\mathbf{r}_2,\ldots,\mathbf{r}_n)=[A-(n-1)]\rho_{n-1}(\mathbf{r}_1,\mathbf{r}_2,\ldots,\mathbf{r}_{n-1};\mathbf{r}_1',\mathbf{r}_2,\ldots,\mathbf{r}_{n-1}). \tag{38}$$

Within the hole approximation, Eq. (38) translates into

$$\int d^3r_n\rho_n^{\mathrm{HA}}(\mathbf{r}_1,\mathbf{r}_2,\ldots,\mathbf{r}_n;\mathbf{r}_1',\mathbf{r}_2,\ldots,\mathbf{r}_n)=(A-1)\rho_{n-1}^{\mathrm{HA}}(\mathbf{r}_1,\mathbf{r}_2,\ldots,\mathbf{r}_{n-1};\mathbf{r}_1',\mathbf{r}_2,\ldots,\mathbf{r}_{n-1}) \tag{39}$$

$$=[A-(n-1)]\rho_{n-1}^{\mathrm{HA}}+O(n-2). \tag{40}$$

In addition to ρ_2, calculation of the generalized folding function in the hole approximation calls for a knowledge of the imaginary part of the quantity $\Gamma_{\mathbf{q}}$ of Eq. (14), i.e., of the imaginary part of the NN scattering amplitude $f_{\mathbf{q}}$. In this work, we have employed the simple parametrization originally proposed in Ref. [19], namely,

$$\mathrm{Im}\,f_{\mathbf{q}}(\mathbf{k})=\frac{|\mathbf{q}|}{4\pi}\sigma_{NN}\exp(-\beta^2|\mathbf{k}|^2). \tag{41}$$

Numerical values of the total NN cross section σ_{NN} and the slope parameter β resulting from fits to NN scattering data are given in Refs. [20] and [21].

Using the hole approximation [Eq. (36)] and together with parametrization (43) of $\mathrm{Im}\,\Gamma_{\mathbf{q}}$, we can finally assemble the working expression

$$F_{\mathbf{k},\mathbf{q}}(\omega)=\frac{1}{n(\mathbf{k})}2\,\mathrm{Re}\frac{1}{v}\int_0^\infty\frac{dz}{2\pi}\exp\left(i\omega\frac{z}{v}\right)\times\int d\mathbf{r}_{11'}e^{i\mathbf{k}\cdot\mathbf{r}_{11'}}E_{\mathbf{q}}(z,\mathbf{r}_{11'}) \tag{42}$$

for the generalized folding function, with

$$E_{\mathbf{q}}(z,\mathbf{r}_{11'})=\exp\left[-\frac{\sigma_{NN}}{16\pi\beta^2}J_{\mathbf{q}}(z,\mathbf{r}_{11'})\right] \tag{43}$$

and

$$J_{\mathbf{q}}(z,\mathbf{r}_{11'})=\frac{1}{\rho_1(r_{11'})}\int_0^\infty r^2dr\int_{-1}^1 d\cos\theta\,\rho_2(r_{11'},r,r')\times\exp\left[-\frac{r^2\sin^2\theta}{4\beta^2}\right]\left[\mathrm{erf}\left(\frac{z+r\cos\theta}{2\beta}\right)-\mathrm{erf}\left(\frac{r\cos\theta}{2\beta}\right)\right]. \tag{44}$$

In the above equations, $\rho_1(r_{11'})$ and $\rho_2(r_{11'},r,r')$, with $r=|\mathbf{r}|=|\mathbf{r}_1-\mathbf{r}_2|$ and $r'=|\mathbf{r}'|=|\mathbf{r}_1'-\mathbf{r}_2|$, are the nuclear-matter one-body and half-diagonal two-body density matrices, respectively, v is the speed of the struck particle, the z axis is chosen along the direction of $\mathbf{q}$, and θ is the angle between $\mathbf{r}$ and $\mathbf{q}$. It can be shown that the $\mathbf{k}$-independent CGA folding function of Ref. [2] can be recaptured from Eqs. (43)–(45) by replacing $\rho_2(\mathbf{r}_1,\mathbf{r}_2;\mathbf{r}_1',\mathbf{r}_2)$ with its fully diagonal part $\rho_2(\mathbf{r}_1,\mathbf{r}_2;\mathbf{r}_1,\mathbf{r}_2)$. The numerical calculation of $F_{\mathbf{k},\mathbf{q}}(\omega)$ has been performed by applying (i) the scheme proposed in Ref. [22] to obtain $n(k)$ and $\rho_1(r_{11'})$ and (ii) the formalism developed in Ref. [23] to evaluate the nuclear-matter half-diagonal two-body density matrix. Both approaches use correlated many-body wave functions and FHNC integral equations to sum up selected cluster contributions to all orders in the relevant expansions.

In particular, $\rho_2(\mathbf{r}_1,\mathbf{r}_2;\mathbf{r}_1',\mathbf{r}_2)$ has been approximated by its leading dd part in the FHNC formalism according to [23]; thus we set

$$\rho_2(\mathbf{r}_1,\mathbf{r}_2;\mathbf{r}_1',\mathbf{r}_2)=\rho_1(r_{11'})g_{Qdd}(r)g_{Qdd}(r'), \tag{45}$$

where $g_{Qdd}(r)$ consists of the dd nodal and non-nodal components of the FHNC expression for $\rho_1(\mathbf{r}_1;\mathbf{r}_1')$. (The notation dd refers to the topological classification of the diagrams associated with the corresponding terms in the cluster expansion. See Ref. [23] for details.)

Due to its weak dependence upon $\cos\phi=\hat{\mathbf{r}}\cdot\hat{\mathbf{r}}_{11'}$, the quantity $g_{Qdd}(r')$ is approximated by its angular average, according to

$$g_{Qdd}(r_1')\to\overline{g}_{Qdd}(r')\equiv\frac{1}{2}\int_{-1}^1 d(\cos\phi)\,g_{Qdd}[(r^2+r_{11'}^2-2rr_{11'}\cos\phi)^{1/2}]. \tag{46}$$

The resulting expression for the generalized folding function is

$$F_{\mathbf{k},\mathbf{q}}(\omega)=\frac{4}{n(\mathbf{k})}\int_0^\infty\frac{dz}{v}\cos\left(\omega\frac{z}{v}\right)\int_0^\infty r_{11'}^2dr_{11'}j_0(kr_{11'})\times\rho_1(r_{11'})\overline{E}_{\mathbf{q}}(z,r_{11'}), \tag{47}$$

where $j_0(x)$ is the zeroth-order spherical Bessel function and

$$\overline{E}_{\mathbf{q}}(z,\mathbf{r}_{11'})=\exp\left[-\frac{\sigma_{NN}}{16\pi\beta^2}\overline{J}_{\mathbf{q}}(z,\mathbf{r}_{11'})\right] \tag{48}$$

with

$$\overline{J}_{\mathbf{q}}(z,\mathbf{r}_{11'})=2\pi\rho\int_0^\infty r^2dr\int_{-1}^1 d\cos\theta\,g_{Qdd}(r)\overline{g}_{Qdd}(r')\times\exp\left[-\frac{r^2\sin^2\theta}{4\beta^2}\right]\left[\mathrm{erf}\left(\frac{z+r\cos\theta}{2\beta}\right)-\mathrm{erf}\left(\frac{r\cos\theta}{2\beta}\right)\right]. \tag{49}$$

IV. NUMERICAL RESULTS

We have carried out the calculation of the nonrelativistic response of a realistic model of nuclear matter, based on the Hamiltonian

$$H=\sum_{i=1}^A\frac{\mathbf{p}^2}{2m}+\sum_{j>i=1}^A v_{ij}+\sum_{k>j>i=1}^A V_{ijk}, \tag{50}$$

where v_{ij} and V_{ijk} are potentials describing two- and three-nucleon interactions, and on a variational ground-state wave function

$$\Psi_0(R)=\mathcal{S}\left[\prod_{i<j}F_{ij}\right]\chi_0(R). \tag{51}$$

In this trial form, $\mathcal{S}$ is a symmetrization operator acting on the product of two-nucleon correlation operators, F_{ij}, and χ_0 is the Slater determinant describing a noninteracting Fermi gas of nucleons with momenta $\mathbf{k}$ filling the Fermi sea, i.e., with $|\mathbf{k}|\leq k_F=(3\pi^2\rho/2)^{1/3}$. The operator F_{ij}, which should reflect the correlation structure induced by the nuclear Hamiltonian, has been chosen as [26]

$$F_{ij}=f_c(r_{ij})+f_\sigma(r_{ij})(\boldsymbol{\sigma}_i\cdot\boldsymbol{\sigma}_j)+f_\tau(r_{ij})(\boldsymbol{\tau}_i\cdot\boldsymbol{\tau}_j)+f_{\sigma\tau}(r_{ij})\times(\boldsymbol{\sigma}_i\cdot\boldsymbol{\sigma}_j)(\boldsymbol{\tau}_i\cdot\boldsymbol{\tau}_j)+f_t(r_{ij})S_{ij}+f_{t\tau}(r_{ij})S_{ij}(\boldsymbol{\tau}_i\cdot\boldsymbol{\tau}_j). \tag{52}$$

Here $S_{ij}=3(\boldsymbol{\sigma}_i\cdot\mathbf{r}_{ij})(\boldsymbol{\sigma}_j\cdot\mathbf{r}_{ij})/|\mathbf{r}_{ij}|^2-(\boldsymbol{\sigma}_i\cdot\boldsymbol{\sigma}_j)$ is the usual tensor operator, while $f_c(r),f_\sigma(r),f_\tau(r),f_{\sigma\tau}(r),f_t(r)$, and $f_{t\tau}(r)$ are correlation functions whose radial shapes are determined by minimizing the expectation value of the Hamiltonian [Eq. (50)] in the ground state described by Eq. (51) [26].

The PWIA response has been calculated using the nucleon spectral function of Ref. [24], obtained from a nuclear Hamiltonian including the Urbana v_{14} *NN* potential supplemented by the TNI model of the three-body interaction [25].

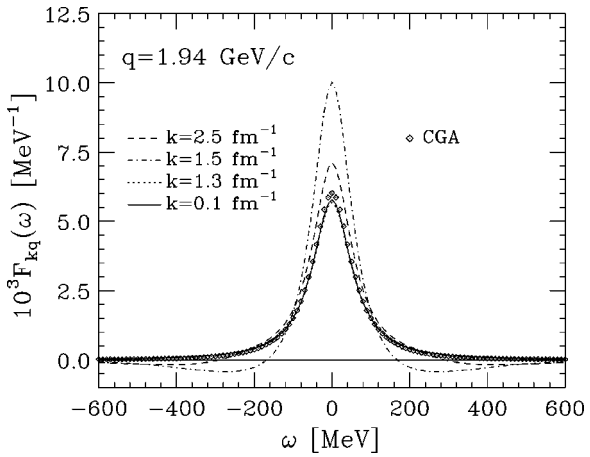

FIG. 1. Dependence of the generalized folding function $F_{\mathbf{k},\mathbf{q}}(\omega)$ of Eqs. (47)–(49) on $k=|\mathbf{k}|$ and ω, at $q=|\mathbf{q}|=1.94$ GeV/c. The diamonds show the results of the approach of Ref. [2], in which the dependence of the folding function upon the initial nucleon momentum **k** is neglected.

The same ingredients entering the calculation of the spectral function have been employed in the calculation of the density matrices needed to obtain the generalized folding function defined by Eqs. (47)–(49).

The dependence of the folding function $F_{\mathbf{k},\mathbf{q}}(\omega)$ on $k \equiv|\mathbf{k}|$ and ω is illustrated in Figs. 1 and 2 at $|\mathbf{q}|=1.31$ and 1.94 GeV/c, two values representative of the range covered by the data analyzed in Refs. [2–4]. For comparison, we also show the k-independent folding functions obtained using the approach developed in I. We note that in symmetric nuclear matter at its equilibrium density $\rho=\rho_0=0.16$ fm^{-3}, the Fermi momentum is $k_F=1.33$ fm^{-1}. It is apparent that in the region $k<k_F$, the folding function $F_{\mathbf{k},\mathbf{q}}(\omega)$ is very close to its CGA counterpart, whereas a strong k dependence is observed at $k>k_F$. At $|\mathbf{k}|\gtrsim k_F$ the generalized folding function shrinks, and its tail begins to oscillate, implying that these k values correspond to weaker FSI. On the other hand, for larger momenta, well above the Fermi level, $F_{\mathbf{k},\mathbf{q}}(\omega)$ becomes broader again. The results of Figs. 1 and 2 confirm the

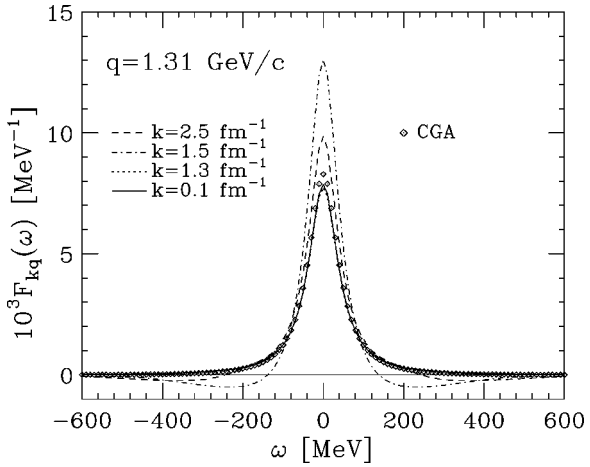

FIG. 2. Same as in Fig. 1, but for momentum transfer $q=|\mathbf{q}|=1.31$ GeV/c.

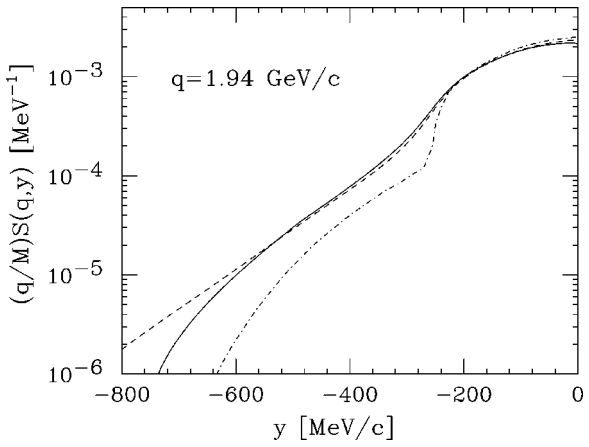

FIG. 3. Dependence of the nuclear-matter scaling function $F(\mathbf{q},y)$ defined by Eqs. (53)–(54) on the scaling variable y, at $q=|\mathbf{q}|=1.94$ GeV/c. The dash-dotted line shows the PWIA result, while the solid and dashed lines correspond respectively to calculations carried out using the generalized folding function of Eqs. (47)–(49) and the $|\mathbf{k}|$-independent CGA folding function of Ref. [2].

naive expectation that while the averaging procedure involved in the approach of Ref. [2] is quite reasonable in the region of $|\mathbf{k}|<k_F$, where the nucleon momentum distribution is nearly constant, the momentum dependence of the folding function associated with fast nucleons, carrying momenta larger than k_F, must be treated explicitly.

Figures 3 and 4 show the dependence of the nuclear matter y-scaling function

$$F(\mathbf{q},y)=\frac{|\mathbf{q}|}{m}S(\mathbf{q},y) \tag{53}$$

on the scaling variable

$$y=\frac{m}{|\mathbf{q}|}\left(\omega-\frac{|\mathbf{q}|^2}{2m}\right), \tag{54}$$

evaluated for the respective choices $|\mathbf{q}|=1.94$ and 1.31 GeV/c of the momentum transfer. Using the y-scaling func-

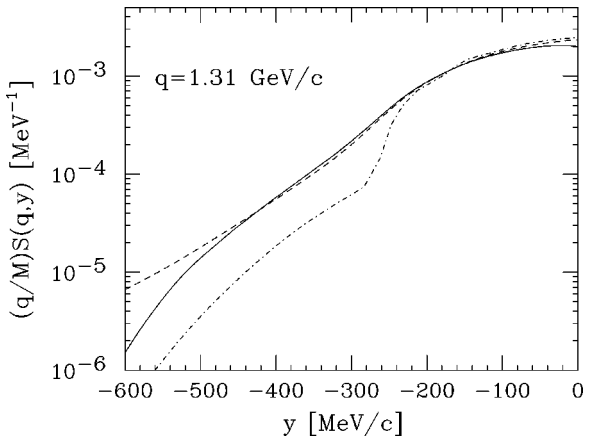

FIG. 4. Same as in Fig. 3, but for momentum transfer $q=|\mathbf{q}|=1.31$ GeV/c.

tion rather than the response makes it easier to directly compare FSI effects at different values of $|\mathbf{q}|$, as measured by the deviation from the PWIA results at fixed y.

Comparison of the PWIA scaling functions (dash-dotted lines) to the results obtained from the CGA (dashed lines) and the approach described in the previous sections (solid lines) clearly demonstrates that use of the **k**-dependent generalized folding function leads to a suppression of FSI effects in the region of large negative y, corresponding to the low-energy tail of the response [see Eq. (54)]. For example, at $y=600$ MeV/c the differences between the dashed and solid lines are $\simeq 70\%$ and $\simeq 20\%$ at $|\mathbf{q}|=1.31$ and 1.94 GeV/c, respectively.

The fact that the suppression of FSI's appears to be more pronounced at the lower values of $|\mathbf{q}|$ indicates that a broader CGA folding function is associated with a smaller effect of the **k** dependence. In fact, the larger value of the *NN* cross section at $|\mathbf{q}|=1.94$ GeV/c, namely $\sigma_{NN}\simeq 43$ mb compared to $\sigma_{NN}\simeq 35$ mb at $|\mathbf{q}|=1.31$ GeV/c, makes the CGA folding function broader at the higher momentum transfer (see Figs. 1 and 2).

V. SUMMARY AND CONCLUSIONS

We have carried out a calculation of the nuclear matter response in which *NN* correlations, which are known to play an important role in the low-energy tail of the response, have been taken into account both in the initial and final states. The effects of dynamical correlations in the initial state have been consistently incorporated into the PWIA calculation, based on a realistic spectral function obtained from an *ab initio* microscopic many-body approach [24].

The same ingredients entering the calculations of the spectral function of Ref. [24] have been employed in the calculation of corrections to the PWIA arising from FSI's between the struck nucleon and the spectator system. Our many-body treatment of FSI's is based on much the same scheme as applied in I and is therefore predicated on the eikonal and frozen approximations. However, the new treatment allows us to go beyond the simple convolution expression for the response and explicitly take into account the dependence on the initial momentum of the struck nucleon, which is averaged over in the CGA.

Numerical results show that the momentum dependence of the generalized folding function produces a sizable effect in the low-energy tail of the y-scaling function in the range of momentum transfer $1<|\mathbf{q}|<2$ GeV/c covered by the inclusive electron-nucleus scattering data analyzed in Refs. [2–4]. While repeating the analysis of Refs. [2–4] within the approach proposed here would certainly be of great interest, it must be pointed out that using a momentum-dependent generalized folding function would in no way help to improve the agreement between the CGA and the data. As shown in I, the discrepancy between the CGA results and the measured cross sections increases as $|\mathbf{q}|$ increases, while the suppression of FSI's due to the momentum dependence of the folding function appears to be larger at lower momentum transfer. A different mechanism, leading to a quenching of FSI's and exhibiting the *opposite* momentum-transfer dependence, such as the one associated with the color-transparency model employed in Refs. [2–4], still seems to be needed to reconcile theory and data.

ACKNOWLEDGMENTS

This research was supported in part by the U.S. National Science Foundation under Grant No. PHY-9900713 (J.W.C.), by the Italian MIUR through the *Progetto di Ricerca di Interesse Nazionale: Fisica Teorica del Nucleo Atomico e dei Sistemi a Molti Corpi* and by the University of Athens under Grant No. 70/3/3309.

[1] *Modern Topics in Electron Scattering*, edited by B. Frois and I. Sick (World Scientific, Singapore, 1991).
[2] O. Benhar, A. Fabrocini, S. Fantoni, G. A. Miller, V. R. Pandharipande, and I. Sick, Phys. Rev. C **44**, 2328 (1991).
[3] O. Benhar and V. R. Pandharipande, Phys. Rev. C **47**, 2218 (1993).
[4] O. Benhar, A. Fabrocini, S. Fantoni, and I. Sick, Nucl. Phys. **A579**, 493 (1994).
[5] J. W. Clark and R. N. Silver, in *Proceedings of the Fifth International Conference on Nuclear Reaction Mechanisms*, edited by E. Gadioli (Università degli Studi di Milano, Milano, 1988), p. 531.
[6] R. J. Glauber, in *Lectures in Theoretical Physics*, edited by W. E. Brittin *et al.* (Interscience, New York, 1959).
[7] A. Bianconi, S. Jeschonnek, N. N. Nikolaev, and B. G. Zakharov, Nucl. Phys. **A608**, 437 (1996).
[8] O. Benhar, N. N. Nikolaev, J. Speth, A. A. Usmani, and B. G. Zakharov, Nucl. Phys. **A673**, 241 (2000).
[9] V. R. Pandharipande and S. C. Pieper, Phys. Rev. C **45**, 791 (1992).
[10] O. Benhar and S. Liuti, Phys. Lett. B **389**, 649 (1996).
[11] S. J. Brodsky, in *Proceedings of the Thirteenth International Symposium on Multiparticle Dynamics*, edited by E. W. Kittel, W. Metzger, and A. Stergion (World Scientific, Singapore, 1982).
[12] A. Mueller, in *Proceedings of the Seventh Rencontre de Moriond*, edited by J. Tran Thanh Van (Editions Frontières, Gif-sur-Yvette, 1982).
[13] G. R. Farrar, H. Liu, L. L. Frankfurt, and M. I. Strikman, Phys. Rev. Lett. **61**, 686 (1988).
[14] O. Benhar, A. Fabrocini, and S. Fantoni, Phys. Rev. Lett. **87**, 052501 (2001).
[15] J. W. Negele and H. Orland, *Quantum Many-Particle Systems* (Addison-Wesley, New York, 1988).
[16] C. Carraro and S. E. Koonin, Nucl. Phys. **A524**, 201 (1991).
[17] O. Benhar, J. Carlson, V. R. Pandharipande, and R. Schiavilla, Phys. Rev. C **52**, 2601 (1995).
[18] A. Akmal and V. R. Pandharipande, Phys. Rev. C **56**, 2261 (1997).

[19] R. H. Bassel and C. Wilkin, Phys. Rev. Lett. **18**, 871 (1967).
[20] A. V. Dobrovolsky *et al.*, Nucl. Phys. **B214**, 1 (1983).
[21] B. H. Silverman *et al.*, Nucl. Phys. **A499**, 763 (1989).
[22] M. F. Flynn, J. W. Clark, R. M. Panoff, O. Bohigas, and S. Stringari, Nucl. Phys. **A427**, 253 (1984).
[23] M. Petraki, E. Mavrommatis, and J. W. Clark, Phys. Rev. C **64**, 024301 (2001).
[24] O. Benhar, A. Fabrocini, and S. Fantoni, Nucl. Phys. **A505**, 267 (1989).
[25] I. E. Lagaris and V. R. Pandharipande, Nucl. Phys. **A359**, 331 (1981).
[26] V. R. Pandharipande and R. B. Wiringa, Rev. Mod. Phys. **51**, 821 (1979).